Nano Scale Disruptive Silicon-Plasmonic Platform for Chip-to-Chip Interconnection

Demonstration and decision on photodetector operation: nano-gap (MIM) vs Schottky/heterostructure

Milestone no.:	MS20
Due date:	04/30/2013
Actual Submission date:	05/13/2013
Authors:	UVEG
Work package(s):	WP4
Distribution level:	RE[1] (NAVOLCHI Consortium)
Nature:	document, available online in the restricted area of the NAVOLCHI webpage

List of Partners concerned

Partner number	Partner name	Partner short name	Country	Date enter project	Date exit project
5	UNIVERSITAT DE VALENCIA	UVEG	Spain	M1	M36

[1] **PU** = Public
PP = Restricted to other programme participants (including the Commission Services)
RE = Restricted to a group specified by the consortium (including the Commission Services)
CO = Confidential, only for members of the consortium (including the Commission Services)

Deliverable Responsible

Organization: University of Valencia Estudi General (UVEG)
Contact Person: Juan P. Martínez Pastor
Address: Instituto de Ciencia de los Materiales, Universidad de Valencia
P.O. Box 22085
46071 Valencia
Spain
Phone: +34 963544793
Fax: +34 963543633
E-mail: martinep@uv.es

Executive Summary

This document shall incorporate (all) rules procedures concerning the technical and administrative management of the project and is therefore to be updated on a regular basis. Please look at www.navolchi.eu regularly for the latest version.

Change Records

Version	Date	Changes	Author
1	2013-05-09		Pedro Rodríguez Cantó
2	2013-05-11	Electro-optical characterization	Juan P. Martínez Pastor
3	2013-05-14		Pedro Rodríguez Cantó
4	2013-05-15	revision	Juan
5			
6			

1. Introduction

The photodetector to be integrated in the plasmonic receiver will consist in a conductive layer of PbS (or PbSe) quantum dots (QDs), whose thickness should be properly optimized, able to generate an electrical current as a response to the incoming photons [1]. Indeed, current literature reports different responsivities depending on the thickness and the design of the detector. For a PbS QD monolayer in a nanogap photoconductor [2] responsivity is in the in the range between 0.1 and 3.9 A/W, but it can be larger than 100 A/W for a PbS film thicker than 200 nm [3] and even more than 10^6 A/W in a MOS structure based on a PbS layer (60-80 nm thick) on graphene [4]. The QD-solid approach is considered one of the latest advanced concepts for photodetection, given the high absorption of quantum dots, the low cost of the solution processing technique used to deposit the material as well as its integration in Si technology. Furthermore, this concept can be easily combined with plasmonic layers based on metal nanoparticles, because a significant enhancement of the responsivity is expected due to light trapping effect at the band edge of the QD-solid [3].

This milestone report deals with the decision on the photodetector operation between two different concepts: QDs deposited on a nano-gap area between the metal contacts or a Schottky-heterostructure design (photodector).

The Schottky photodiode concept is a robust design and easy fabrication, can work without bias (photocurrent/photovoltage mode) with responsivities of the order of 1 A/W or more using negative bias, but the footprint is larger, worse time response and it will be more difficult to integrate with planar photonics technology.

The nano-gap design can have many advantages:

i) small footprint,
ii) small bias voltage,
iii) fast operation and
iv) plasmonic effects can play a role for signal enhancement due to the small separation between metal contacts (antenna effect),

but it also has important disadvantages, as the low electric signal expected due to the small area for photon capture and the challenging fabrication.

The micro-gap is a design similar to that of the nano-gap, but it can be fabricated easily (photolithography instead of ebeam lithography). The most important advantage is the reasonably small footprint, it can be easily integrated with planar photonics technology, and big electric signal (high photoconductive gain as aforementioned) and fast operation can be reached depending upon bias voltage. The main disadvantage can be the high bias voltage needed for optimal signal and fast operation.

To demonstrate the feasibility and performance of the mentioned architectures proposed in this project, we have accomplished following outcomes so far:

- Preparation of QD-solids, experimental details, and optical characterization.
- Electro-optical properties of Schottky/heterostructure photodetectors. *Good results.*
- Electro-optical properties of micro-gap photoconductors. *Preliminary results.*
- Electro-optical properties of nano-gap photoconductors. *Under development.*

2. Preparation of QD-solids and experimental devices

The synthesis of QDs for IR has been described in detail in Milestone-18 and Deliverable 4.2. Briefly, this synthesis is based on the hot injection of metal-organic precursors into coordinating/non-coordinating solvents at elevated temperatures. The synthesis of PbS (and PbSe) QDs is developed by the spin-off company of the UVEG group. A ligand exchange reaction after the synthesis is carried out by dispersing oleate-capped PbS in oleylamine, which has the same molecular size as oleic acid but exhibits less affinity to PbS. In this way, the bond between PbS and oleylamine is weaker than that of PbS and oleate, as required for the subsequent formation of the QD solid, as described below. After this first ligand exchange, absorption is blue-shifted by 10 nm. Finally, QDs are redispersed in octane at a concentration of 20 mg/mL, which is the typical concentration used for the layer stack formation.

The production of QD-solids is based on a solution-processing method called Layer-by-Layer (LbL), also extensively described in Milestone-18 and Deliverable 4.2. This approach allows the fabrication of smooth and crevice-free QD films directly from the colloidal solution. The key step of this method consists in a ligand exchange reaction to replace the insulating oleyamine (2 nm long) for shorter ligands. The ligand used in the present work is bidentate in order to closely interconnect QDs. Among the bidentate ligands tested for the fabrication of layer stacks, we decided to start investigating 3-Mercaptopropionic acid (MPA) instead of ethanedithiol (EDT), thioglicolic acid or oxalic acid, since MPA provides greater chemical diversity in comparison to EDT and is thus able to passivize a broader distribution of surface states [5].

PbS QD films were typically deposited on glass (for micro-gap photoconductors), glass-ITO (thin) (for nano-gap photoconductors) or glass/ITO/PEDOT (for Schottky/heterostructure photovoltaic photodetectors) substrates through the LbL spin-coating process. Each iteration in the layer-by-layer deposition consisted of five steps: 1) 5 drops of PbS solution in octane; 2) 5 drops of a 1% bidentate ligand solution (3-Mercaptopropionic acid (MPA); 3) 10 drops of methanol; 4) 10 drops of anhydrous octane; 5) 10 s hair dryer hot air-dry. We repeat these steps 8-14 times to obtain smooth quantum dot films 230-360 nm thick, as measured by a mechanical profilometer.

Figure 1 shows the absorbance and PL spectra of a MPA-capped PbS QD film with a thickness of around 280 nm (corresponding to 12 layer depositions). The optical properties were preserved after ligand exchange, even if the quantum yield of photoluminescence decreases accordingly to the shortening of organic ligands between QDs (this was measured in QD-solids based on CdSe QDs emitting at 600 nm).

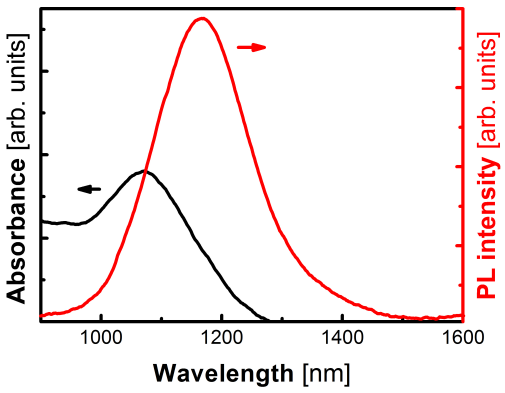

Figure 1: Absorption and PL spectra of MPA-capped PbS film.

The surface roughness of LbL films has been measured by using a mechanical profilometer. The resulting surface roughness of a 360 nm film was about 15 nm in average, as depicted in Fig. 2. This value means less than 5 % of the total film thickness, but it could locally influence negatively the electrical properties of devices. To minimize that, the first simple solution will be to increase the thickness of the QD-solid film. In fact, photocurrent measured on photodiodes based on QD films 360 nm thick (14 LbL-cycles) are 4-5 times better than those made on QD films 230 nm thick (8 LbL-cycles), as reported below. Nevertheless, the LbL method followed here is relatively time-consuming to produce thick layers by spin-coating, without using an automatic dispensation of the QD solution. An alternative method to be considered in next future to produce QD films with smaller surface roughness will be dip-coating (see Ref. 1 and others therein). For this purpose we have developed an automated homemade dip-coater, in parallel to the device fabrication based on the LbL method by spin-coating.

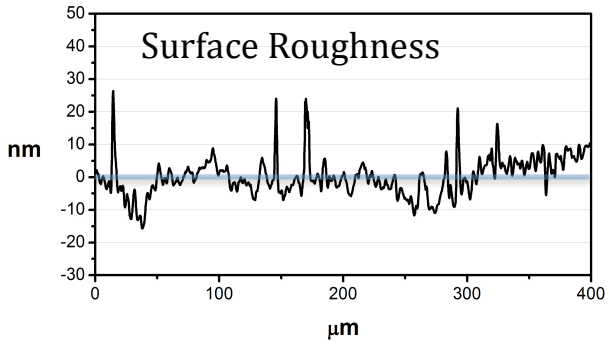

Figure 2. Surface roughness measured by profilometry in a 360 nm thick PbS QD film.

Previous studies in literature on PbS photoconductors have reported that photosensitization of PbS is followed by oxidation, and in particular formation of lead sulfates ($PbSO_4$) and/or lead sulphites ($PbSO_3$) [6]. They act as sensitizing centres that prolong the minority (electron) carrier lifetime allowing holes to transverse the device within this carrier lifetime. We maintain this hypothesis, but further studies will be developed to determine the generation/recombination mechanism in our material. For the moment, we have established a technological processing, as described above, for a reproducible preparation of QD solids. These layers and devices maintain their good electro-optical properties stable in air during weeks. They exhibit photoconductive properties as shown below, even if we still continue to work actively on the chemistry to improve the optical quality of the IV-VI QDs. This is necessary for understanding the physics of the device and introducing surface traps for electrons in a controlled way, if necessary.

To measure the electro-optical properties of the photodevices we have developed an in-house set-up based on la Xe-lamp (150 W) and monochromator 300 mm of focal length for illumination, a low-noise pre-amplifier and/or lock-in electronics for electrical signal amplification, other than a calibrated Si-photodiode to obtain responsivity values in the region 350-1100 nm. In parallel, we also use a Keithley 2400 source-meter for measuring I(V) characteristics under dark or illumination conditions (monochromatic light). The monochromatic light leaving the monochromator is focused onto the device transparent surface (from glass substrate) through a 20x objective. Then, we are able to measure weak and intermediate/large photocurrent signals by using the first and second type of measurements, respectively.

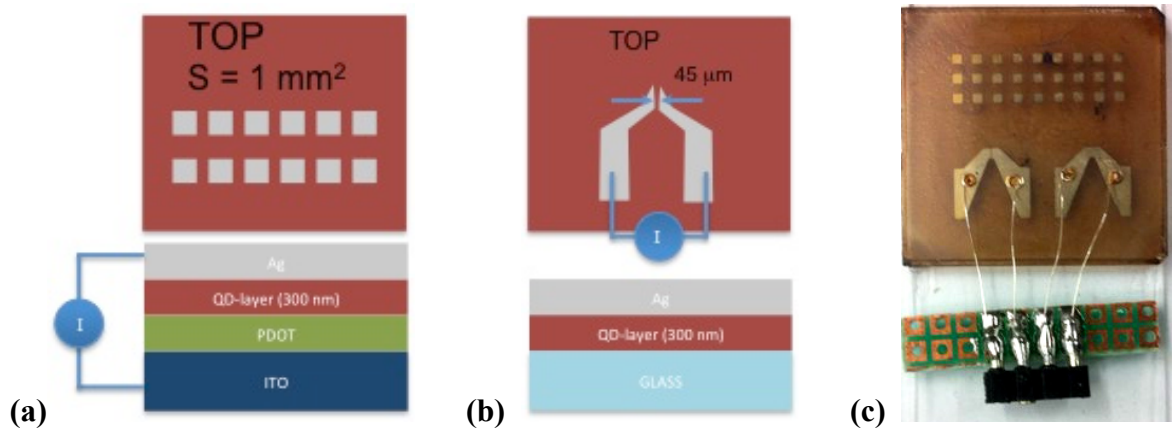

Figure 3. Schottky/heterostructure photodiodes (a) and micro-gap photoconductor (b). Mask used for the Ag electrode deposition is the same for both designs (c); in the example contacts are made on the photoconductive design.

For the present study, the deposition of metal electrodes was made by using a resistive thermal evaporator and the masks fabricated by laser patterning on aluminum foil (resolution around 5 µm). For Schottky photovoltaic photodetectors (Fig. 3.a) we are using glass/ITO commercial substrates with standard 10-20 Ω.sq resistivity. A thin (100 nm) PEDOT layer is covering the ITO layer by spin-coating in order to reduce the ITO surface roughness and avoid shortcuts by high electric field conditions. The LbL QD-solid is deposited after the PEDOT layer formation and the structure is finished by a top metal contact, for which we are using Ag. For micro-gap photoconductors (Fig. 3.b) we are using glass substrates where LbL QD-solid is deposited directly on glass and the same electrode (Ag) on top. The deposition of top Ag electrodes (100 nm thick) was performed at 3-4 Å/s by thermal evaporation using a Mo boat. Figure 3.c shows the picture of a contacted (silver wires glued with silver epoxy on evaporated contacts) micro-gap (45 ± 5 µm) photoconductor device; the electric field in these micro-gap photoconductors will be in the order of 22 kV/m for 1 V bias. In Schottky photodetectors the 1 mm^2 square Ag patterns (Fig. 3.c) are contacted for electro-optical characterization.

3. Electro-optical properties of Schottky/heterostructure photodetectors.

In Schottky photodiodes (Fig. 3.a) we have characterized the I(V) characteristics under dark and illumination conditions at different wavelengths, as plotted in Fig. 4. Clearly, they are limited by a series resistance of the order of 2500 Ω, even smaller for higher bias, which yields ρ = 7.10^5 Ω.cm if we attribute that series resistance to the resistivity of the PbS QD film. This resistivity is consistent with that obtained in micro-gap devices, as reported below, and not far from literature data [7]. As aforementioned, thicker and less rough films will help in improving the dark I(V) curve of Schottky diodes [8]. Further improvement could be attained if using metals with higher work function for the top metal electrode, as the case of Al [9] and LiF thin layer between the QD film and the metal electrode to improve the Schottky contact [10]. Given the limitation imposed by the series resistance of the diode the resulting open circuit voltage, V_{OC}, filling factor and efficiency (8.5 mV, 0.28 and 0.3 % at 560 nm, respectively, for an incident power of 4.4 µW) are seriously compromised, as observed in Fig. 4. Photocurrent (short

circuit current), reaches reasonable values, given that responsivity ($R = I_{ph} / P_i$) reaches high values at visible wavelengths where most of the incident flux can be absorbed by the QD film (see black dashed line in Fig. 5).

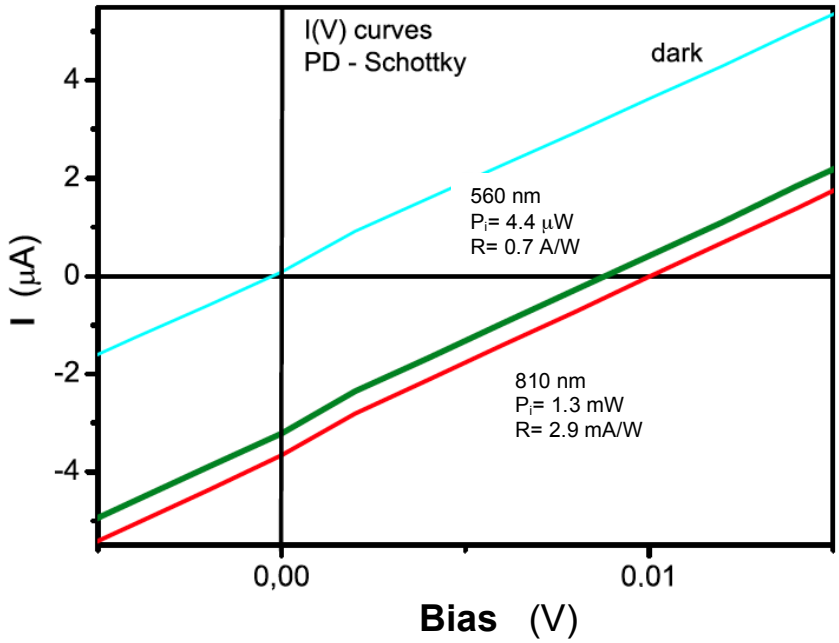

Figure 4. I(V) characteristics of the best ITO/PDOT/PbS-QD-solid(360 nm)/Ag photodiode under dark (cyan line) and illumination at 560 (green line) and 810 (red line) nm.

The responsivity curves measured in different PbS-QD Schottky photodiodes (different synthesis, QD film thickness from 230 to 360 nm) are well correlated with the absorbance, except in the region of the first excited state absorption (750-900 nm), where *R* is proportionally smaller than above and below this region (Fig. 5). This effect could be tentatively attributed to some efficient transfer of majority carriers towards defects. For wavelengths shorter than 500 nm the responsivity decreases, possibly because of the more importance surface recombination effect due to the growing absorption at the PDOT/QD-film interface.

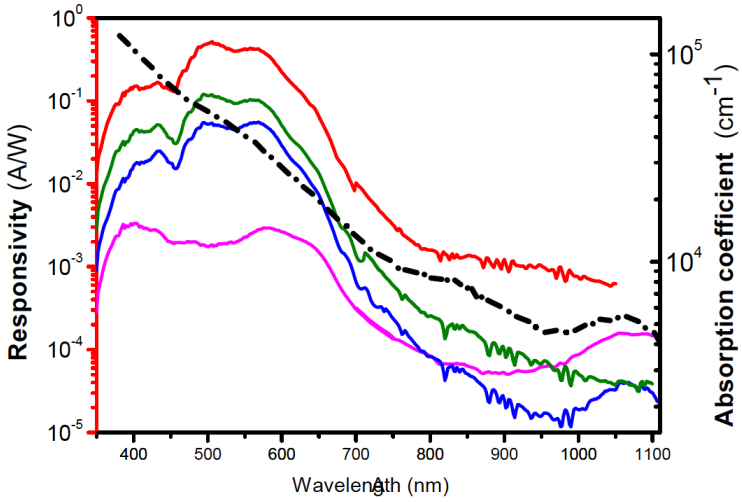

Figure 5. Responsivity curves measured in different glass/ITO/PEDOT/QD-film/Ag Schottky photodiodes (colour continuous lines) compared to absorbance (red line) spectrum in a sample 230 nm thick.

The highest responsivity curve (red curve in Fig. 5) was reached in the case of photodiodes prepared for the thickest QD-solid film (360 nm) and using PbS QDs synthesized with excess of Pb. This curve was measured in one of the photodiodes in the same day of fabrication and was the best of six (differences of a factor 2-4 were appreciated). Surprisingly, after several weeks, the differences in the maximum photocurrent and photocurrent spectra between those photodiodes practically disappeared, as observed in Fig. 6. The highest Responsivity, $R = 0.7\ A/W$, takes place at around 520 nm, whereas decreases up to 1 mA/W at the region close to the PbS QD-film absorption edge. The maximum responsivity corresponds to an EQE ≈ 1 that means all absorbed photons are contributing to charge generation, whereas at the infrared $\alpha d << 1$ and hence the EQE decreases significantly (10^{-3} at 900 nm). Again, thicker films would lead to better results, now regarding absorption and signal at infrared wavelengths.

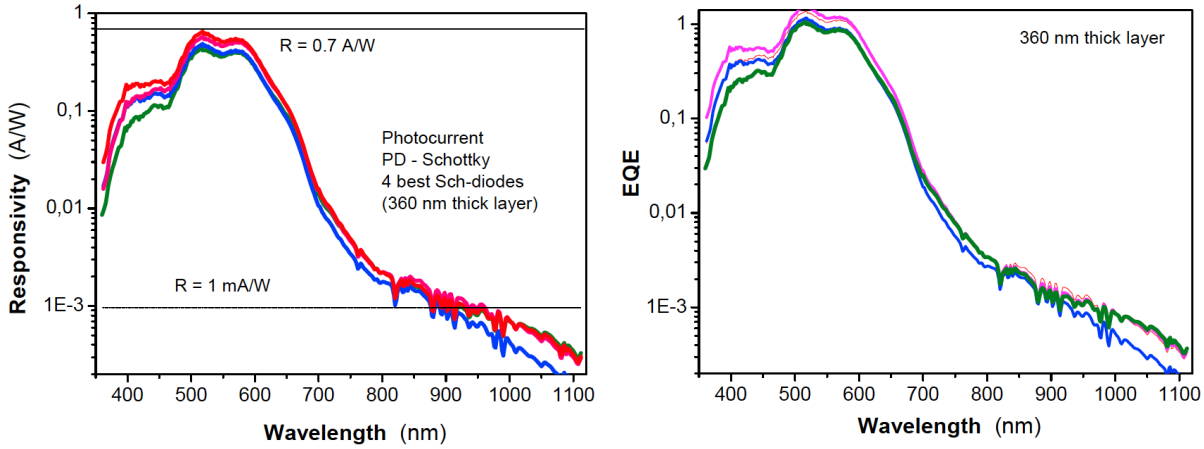

Figure 6. Responsivity spectra (left) and External Quantum Efficieny (right), EQE, measured in different glass/ITO/PEDOT/QD-film/Ag photodiodes of the same sample.

In parallel to this work, in the group we are developing the deposition of ZnO transparent (Fig. 7, left) and conductive layers by a sol-gel method that can be also of interest for improving the Schottky contact with QD films (see for example Ref. 11). This film is polycrystalline and can serve as a seed layer for a posterior growth of ZnO nanowires (Fig. 7, centre) to improve the surface in contact with active layers. Furthermore, the seed layer can be deposited by spin-coating and micro-dispensing (Fig. 7, right). At the moment we are optimizing the resistivity of the layers by annealing process at high temperatures.

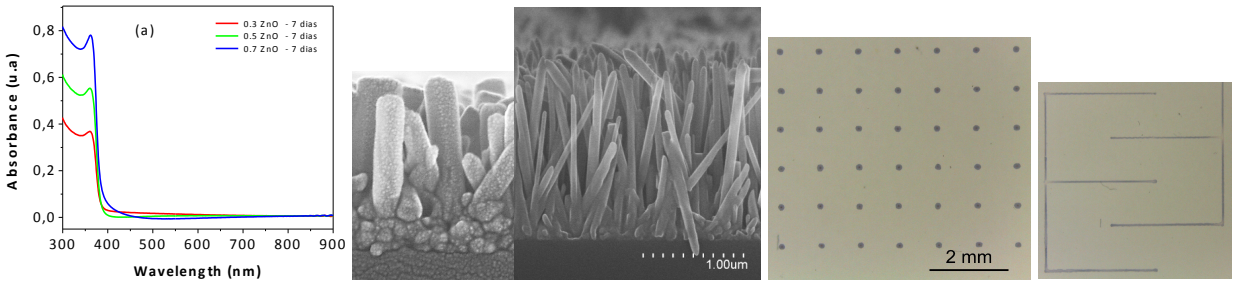

Figure 7. Optical absorption of the a ZnO layer deposited on quartz by a sol-gel method for different concentrations of the Zn precursor (left); ZnO nanowires grown by wet chemistry onto a ZnO layer seed produced by sol-gel (centre); ZnO seed layer deposited by micro-dispensing as disks and lines (right).

4. Electro-optical properties of nano-gap and micro-gap photoconductors.

Photoconductive gain of QD-solids can be very high, in the range of several hundreds to several thousands [12] and even millions in the case of hybrid graphene/QD-solid device [4], being the reason to consider photoconductors in Navolchi. The idea to consider a nano-gap separation between electrodes on the QD film was to reduce the response time for fast operation receivers and combine with plasmonic effects due to the small separation between metal contacts (antenna effect). In a recent publication, where a single QD monolayer was deposited between the electrodes, the time response could be limited by tunneling (i.e., in the subpicosecond regime) [2]. Evidently, a nano-gap device with such a short distance between electrodes (5 nm) is very challenging technologically, other than the problem of having sufficiently high electrical signal to measure low light levels.

Given that technical difficulty to achieve nano-gap distances and the possible difficulties to couple sufficient light leaving the plasmonic amplifier into this photoconductive device, we also considered the study of micro-gap photoconductors (Fig. 3.b-c). First devices were made with an electrode-to-electrode distance ≈ 45 μm. The resistance measured in the 1 V range was around 1 GΩ in a QD film 300 nm thick (12 LbL cycles), that is, a resistivity of 7.10^5 Ω.cm, equal to that estimated in a photodiode configuration through its series resistance losses.

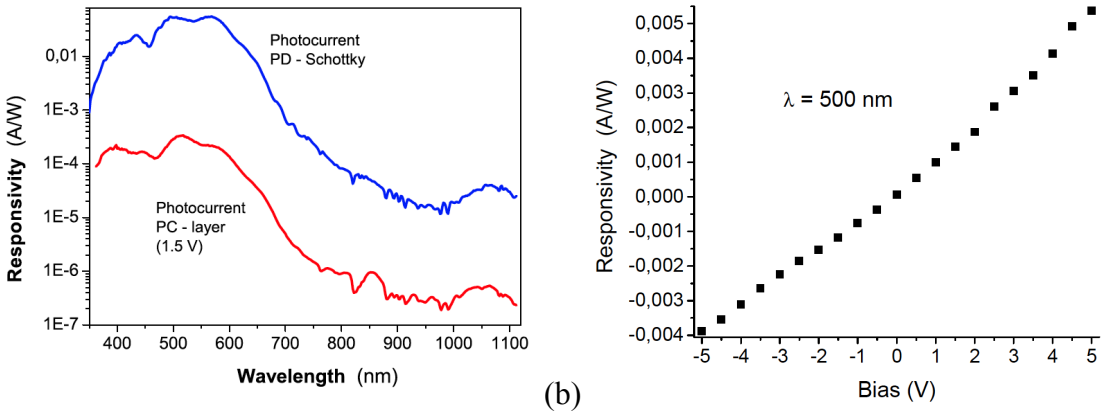

Figure 8. (a) Responsivity curve of a PbSe QD-solid micro-gap photoconductor (red line) 280 nm thick as compared to that measured through the short circuit photocurrent in a glass/ITO/PEDOT/QD-film(280 nm)/Ag photodiode (blue line); (b) Responsivity as a function of applied bias in the same micro-gap photoconductor at 500 nm.

The responsivity curve of a micro-gap photoconductor (45 μm distance between electrodes) measured at 1.5 V bias is about 2 orders of magnitude below that of a Schottky photodiode made on a PbS QD film with similar thickness and preparation conditions (Fig. 8.a). Such a difference can be attributed to the still long distance between electrodes as compared to diffusion length of the material and the small in-plane electric field (even if these responsivity values are a low limit, by assuming that the whole exit slit of the monochromator is focused between the photoconductor electrodes). In fact, illuminating at a single wavelength (500 nm) and double incident optical power the responsivity increases up to 5.5 mA/W at +5 V, as observed in Fig. 8.b, that is, near a factor 20 higher than that shown in Fig. 8.a. On the other hand, It must be said that high bias leads to a proportional photocurrent quenching possibly due to still not completely

cured QD-solid (the curve in Fig. 8.b was recorded in several seconds immediately after illumination). This effect is present in Schottky photodiodes too, but not so important, possibly because of the QD film surface metallization as compared to the air free surface in the micro-gap photoconductor. In any case, this is a solvable problem by a better curing of the QD film and possible an additional passivation using a capping/encapsulating layer of PMMA, for example.

5. Conclusions and further work

PbS and PbSe QDs are synthesized with appropriate diameters to obtain ground exciton absorption in the near infrared (1000 – 1900 nm). QD solids based on PbS have been prepared in a reproducible way, exhibiting oxides at the QD surface and stable in air, as the photodevices fabricated with them. In fact, after several weeks in air the electro-optical properties of devices are better than those recorded under pristine conditions. Furthermore, these properties are less sensitive to applied bias and carrier photo-injection rate that is attributed to a slow curing of the QD-solid at room temperature, even if a curing process is performed after the LbL process during 30-60 min at 100-110 ºC.

Photodiode devices exhibit appropriate photo-electrical properties for light detection in a wide range of wavelengths: they exhibit a high maximum responsivity of 0.7 A/W and EQE ≈ 1. Therefore, these photodiodes are ready to be used as photodetectors once improved sensitivity at infrared wavelengths: use of PbS (or PbSe) with effective bandgap at λ_g > 1550 nm and thicker QD-solid films. These devices can work under both photocurrent and photovoltage (short-circuit current / open-circuit voltage) modes. Electrical characteristics would be improved, even if they do not compromise the photocurrent operation (only reduces the photovoltage signal due to series resistance effect).

Using micro- and nano-gap separated electrodes much important photoconductive gain (see advantages and disadvantages exposed in the introduction) is expected after improving the QD-solid curing and/or its surface isolation (in photodiodes the surface is covered by the metal electrode). Preliminary results in micro-gap devices with 45 μm distance between electrodes are not giving such expected high photoconductive gain values, possibly because this distance is large in comparison to diffusion length. In fact, photoconductive devices in literature uses distances in the range 5 – 15 μm.

Further work and improvements:

- Preparation of devices with QD-solids to have absorption and good responsivity at 1550 nm: optimization of layer thickness and surface roughness.
- Optimization of Schottky/heterostructure photodiodes: use of Al as metal electrode [1] and ZnO instead of ITO (or ITO/ZnO) [11].
- Use of other ligands between QDs [12].
- Optimization of separation between lateral electrodes in the μm-range (micro-gap photoconductors): 2 – 10 μm [2].
- Fabrication and characterization of nano-gap photoconductors.

References

[1] G. Konstantatos and E.H. Sargent, "Nanostructured materials for photodetection", Nature Nanotechnology, 5, 391-
[2] F. Prins, M. Buscema, J. S. Seldenthuis, S. Etaki, G. Buchs, M. Barkelid,V. Zwiller, Y. Gao, A. J. Houtepen, L. D. A. Siebbeles, and H. S. J. van der Zant, "Fast and Efficient Photodetection in Nanoscale Quantum-Dot Junctions", *Nanolett.* **12**, 5740-5743 (2012).
[3] F. Pelayo García de Arquer, F. J. Beck, M. Bernechea, and G. Konstantatos, "Plasmonic light trapping leads to responsivity increase in colloidal quantum dot photodetectors", *Appl. Phys. Lett.* **100**, 043101 (2012).
[4] G. Konstantatos, M. Badioli, L. Gaudreau, J. Osmond, M. Bernechea, F. Pelayo Garcia de Arquer, F. Gatti and F. H. L. Koppens, "Hybrid graphene–quantum dot phototransistors with ultrahigh gain", *Nat. Nanotech.* 7, 363–368 (2012).
[5] Kwang S. Jeong, Jiang Tang, Huan Liu, Jihye Kim, Andrew W. Schaefer, Kyle Kemp, Larissa Levina, XihuaWang, Sjoerd Hoogland, Ratan Debnath, Lukasz Brzozowski, Edward H. Sargent, and John B. Asbury, "Enhanced Mobility-Lifetime Products in PbS Colloidal Quantum Dot Photovoltaics", *ACS Nano* 6 (1), 89–99 (2012).
[6] Jiang Tang, Lukasz Brzozowski, D. Aaron R. Barkhouse, Xihua Wang, Ratan Debnath, Remigiusz Wolowiec, Elenita Palmiano, Larissa Levina, Andras G. Pattantyus-Abraham, Damir Jamakosmanovic, and Edward H. Sargent, "Quantum Dot Photovoltaics in the Extreme Quantum Confinement Regime: The Surface-Chemical Origins of Exceptional Air- and Light-Stability", ACS Nano **4**, 869-878 (2010).
[7] J. M. Luther, M. Law, Q. Song, C. L. Perkins, M. C.Beard, and A. J. Nozik, "Structural, Optical, and Electrical Properties of Self-Assembled Films of PbSe Nanocrystals Treated with 1,2-Ethanedithiol", ACS Nano **2**, 271−280 (2008).
[8] S. Hinds, L. Levina, E. J. D. Klem, G. Konstantatos, V. Sukhovatkin, and E. H. Sargent, "Smooth-Morphology Ultrasensitive Solution-Processed Photodetectors", *Adv. Mater.* **20**, 1–5 (2008).
[9] J.P. Clifford, G. Konstantatos, K.W. Johnston, S. Hoogland, L. Levina, and E.H. Sargent, "Fast, sensitive and spectrally tuneable colloidal-quantum-dot photodetectors", *Nature Nanotechnology* **4**, 40-44 (2009).
[10] R. Debnath, J. Tang, D. A. Barkhouse, X. Wang, A. G. Pattantyus-Abraham, L. Brzozowski, L. Levina, and E. H. Sargent, "Ambient-Processed Colloidal Quantum Dot Solar Cells via Individual Pre-Encapsulation of Nanoparticles", J. Am. Chem. Soc. 132, 5952–5953 (2010).
[11] O. E. Semonin, J. M. Luther, S. Choi, H.-Yu Chen, J. Gao, A. J. Nozik, and M. C. Beard, "Peak External Photocurrent Quantum Efficiency Exceeding 100% via MEG in a Quantum Dot Solar Cell", *Science* **334**, 1530 (2011).
[12] C. Hu, A. Gassenqa, Y. Justo, S. Yakunin, W. Heiss, Z. Hens, G. Roelkens, "Short-wave Infrared Colloidal Quantum Dot Photodetectors on Silicon", *Proc. SPIE* 8631, Quantum Sensing and Nanophotonic Devices X, 863127; doi:10.1117/12.2001246 (February 4, 2013).